# AB INITIO CALCULATIONS OF THE ELECTRONIC STRUCTURE AND OPTICAL PROPERTIES OF CU<sub>4</sub>SeTe Crystals

K. K. AZIZOVA <sup>1,2,3</sup>, Z. A. JAHANGIRLI <sup>1,4,5</sup>, S. S. RAGIMOV <sup>1,4</sup>, T. K. NURUBEYLI <sup>1,6,7\*</sup>, L. CH. SULEYMANOVA<sup>8</sup>, N. V. KERIMLI<sup>9</sup>, G. N. MAMMADOVA <sup>10</sup>, L. V. MAMMADOV <sup>11</sup>, S. O. GULIEVA <sup>12</sup>

- <sup>1</sup> Institute of Physics, Ministry of Science and Education of the Republic of Azerbaijan, Baku, AZ1073, Azerbaijan
- <sup>2</sup> Azerbaijan University, 71 Jeyhun Hajibeyli Str., Baku AZ1007, Azerbaijan
- <sup>3</sup> Western Caspian University, 31 Istiglaliyyat Str., Baku AZ 1001, Azerbaijan
- <sup>4</sup> Baku State University, 23 Academic Zahid Khalilov Str., AZ 1148. Baku, AZ-1073/1, Azerbaijan
- <sup>5</sup> CMD-AC UNEC Research Center, Azerbaijan State University of Economics (UNEC), 6 Istiqlaliyyat Str., Baku, AZ-1001 Azerbaijan
- <sup>6</sup> Azerbaijan State Oil and Industry University, 20 Azadliq Avenue, Baku, AZ-1010, Azerbaijan
- <sup>7</sup> Khazar University, 41 Mahsati Str., Baku, AZ 1096, Azerbaijan.
- 8 Mingachevir State University, 22 Dilara Aliyeva Str., Mingachevir, Az 4500, Azerbaijan
- <sup>9</sup> Azerbaijan Medical University, 167 Samad Vurgun Str., Baku Az1022, Azerbaijan
- 10 Nakhchivan State University, Nakhchivan, University Campus, AZ 7012, Nakhchivan, Azerbaijan
- <sup>11</sup>Baku Engineering University, Khirdalan city, 120 Hasan Aliyev Str., AZ0101, Absheron, Azerbaijan
- <sup>12</sup> Academy of Public Administration under the President of the Republic of Azerbaijan,74 Lermontov Str., Baku, AZ1001, Azerbaijan
- \* Correspondent author: samire.quliyeva.1505@gmail.com

Received: 03.08.2025

**Abstract.** In this study, we present a comprehensive theoretical exploration of the electronic structure and optical properties of  $Cu_4SeTe$  crystals using first-principles density functional theory (DFT) calculations. The analysis covers band structure, total and partial density of states (DOS and PDOS), complex dielectric function, refractive index, extinction coefficient, reflectivity, absorption coefficient, and optical conductivity. The results show that  $Cu_4SeTe$  behaves as a semimetal with hybridized  $Cu_3d$  and  $Se/Te_3e$  p states dominating the valence region, while  $Cu_3e$  and  $Cu_3e$  p states form the conduction bands. The optical spectra calculated reveal strong absorption in the visible range (2–4 eV), with absorption coefficients reaching approximately  $Cu_3e$  and optical anisotropy. These findings suggest that  $Cu_4e$  is a promising multifunctional material with potential applications in thin-film photovoltaics, photodetectors, and thermoelectric devices.

**Keywords:** Cu<sub>4</sub>SeTe, *ab initio* calculations, optical properties, density of states, dielectric function, absorption coefficient, reflectivity

UDC: 538.9; 535; 621.315.592

DOI: 10.3116/16091833/Ukr.J.Phys.Opt.2025.04049

This work is licensed under the Creative Commons Attribution International License (CC BY 4.0).

# 1.Introduction

Copper chalcogenides are a broad and versatile group of materials characterized by variable valence states, diverse crystal structures, high ionic mobility, and rich defect chemistry. These distinctive features have made them appealing candidates for a wide range of technological applications, including photovoltaics, solid-state ionics, phase-change memory, photodetectors, and thermoelectric devices [1–3]. Notably, mixed-anion compounds offer additional flexibility for tuning structural, electronic, and transport properties. Among these,  $Cu_4SeTe$  has recently attracted attention due to its intermediate position between the well-known binary compounds  $Cu_2Se$  and  $Cu_2Te$ .

Cu<sub>2</sub>Se and Cu<sub>2</sub>Te are widely studied materials that crystallize in cubic and lower-symmetry phases, respectively. They are known for their polymorphism and superionic behavior. Cu<sub>2</sub>Se, with its exceptionally low lattice thermal conductivity, has been extensively investigated as a high-performance thermoelectric material [4], while Cu<sub>2</sub>Te shows favorable electrical conductivity and stability. Combining Se and Te into a single ternary compound, such as Cu<sub>4</sub>SeTe, is expected to create a unique balance of high electrical conductivity, an increased Seebeck coefficient, and lower thermal conductivity due to phonon scattering by the heavier Te atoms [5]. This makes Cu<sub>4</sub>SeTe a potentially promising material for thermoelectric and optoelectronic applications.

Despite the increasing interest in copper-based chalcogenides, Cu<sub>4</sub>SeTe remains relatively underexplored, especially concerning its electronic structure and optical properties [6–8]. Only a few experimental studies are available, and systematic first-principles research is lacking. In recent years, ternary copper chalcogenides have gained renewed attention for advanced energy-related applications due to their adjustable band structures, strong light absorption in the visible and near-infrared regions, and compatibility with low-cost thin-film fabrication methods [9–11]. Materials like Cu<sub>2</sub>ZnSnS<sub>4</sub>and Cu<sub>3</sub>SbSe<sub>4</sub> are already being actively studied as absorber layers in photovoltaic devices; however, the Cu–Se–Te system provides additional opportunities to tune band alignment, optical response, and carrier transport.

The present study aims to fill this knowledge gap by providing a detailed theoretical analysis of the electronic structure and optical properties of Cu<sub>4</sub>SeTe based on density functional theory (DFT). The calculations encompass electronic band dispersion, total and partial densities of states, as well as a comprehensive set of optical parameters, including dielectric function, refractive index, extinction coefficient, reflectivity, absorption coefficient, and optical conductivity. These results not only provide fundamental insight into the physics of Cu<sub>4</sub>SeTe but also serve as a guide for future experimental investigations. The outcomes highlight the potential of Cu<sub>4</sub>SeTe as a multifunctional material for thin-film photovoltaics, broadband photodetectors, and thermoelectric energy converters [12].

## 2.2. Results and discussion

#### 2.1. Electrical transport properties

Fig. 1 shows the temperature dependence of the electrical conductivity and Seebeck coefficient of  $Cu_4SeTe$ , measured in the range of  $80-320 \, \text{K}$ . The electrical conductivity decreases slightly with increasing temperature, characteristic of semimetallic behavior. This

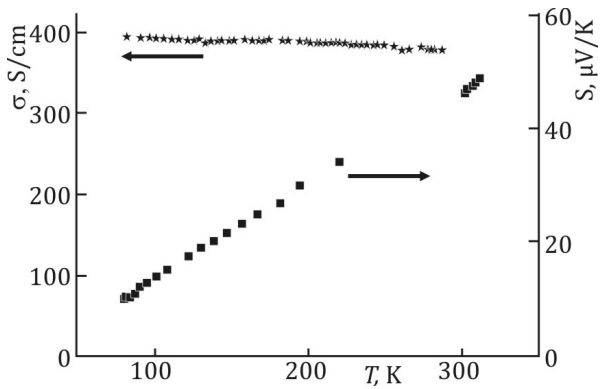


**Fig. 1.** Temperature dependence of electrical conductivity (stars) and Seebeck coefficient (squares) for Cu<sub>4</sub>SeTe.

trend is typically associated with a high carrier concentration, where the dominant scattering mechanisms at elevated temperatures reduce mobility only moderately. The magnitude of conductivity (~720 S/cm at 300 K) positions Cu<sub>4</sub>SeTe between Cu<sub>2</sub>Se and Cu<sub>2</sub>Te, confirming its intermediate transport character.

The Seebeck coefficient consistently rises with temperature and

stays positive across the entire studied range, confirming p-type conduction. At room temperature, its value reaches about 170  $\mu$ V/K, which is similar to that of Cu<sub>2</sub>Te but slightly lower than Cu<sub>2</sub>Se. This behavior shows that Cu<sub>4</sub>SeTe combines the favorable transport features of both binary compounds, balancing conductivity and thermopower.

Hall effect measurements further support this interpretation, revealing a hole mobility of approximately  $20\,\mathrm{cm^2/V}\times\mathrm{s}$  at room temperature. This relatively moderate mobility, combined with the observed Seebeck coefficient, indicates that carrier scattering is affected by the layered structure of the compound and the presence of both Se and Te anions. The combination of high conductivity, moderate Seebeck coefficient, and layered crystal structure suggests increased phonon scattering, which is beneficial for lowering lattice thermal conductivity and enhancing thermoelectric performance.

These experimental results provide the first systematic transport characterization of Cu<sub>4</sub>SeTe, demonstrating that its electronic properties are consistent with those of a semimetallic system. They also form a solid basis for interpreting the theoretical results discussed below.

# 2.2. Electronic band structure and density of states

To further clarify the electronic behavior of Cu<sub>4</sub>SeTe, first-principles calculations based on density functional theory (DFT) were performed using both GGA and GGA+U approximations. Fig. 2 shows the calculated electronic band structures. In both cases, the material displays semimetallic behavior, which aligns well with the measured transport properties. The inclusion of the Hubbard U correction shifts the Cu 3d bands to lower energies relative to the Fermi level, but the overall semimetallic nature of the compound remains the same. This finding is consistent with other copper-based layered chalcogenides, where narrow d-bands coexist with delocalized conduction states.

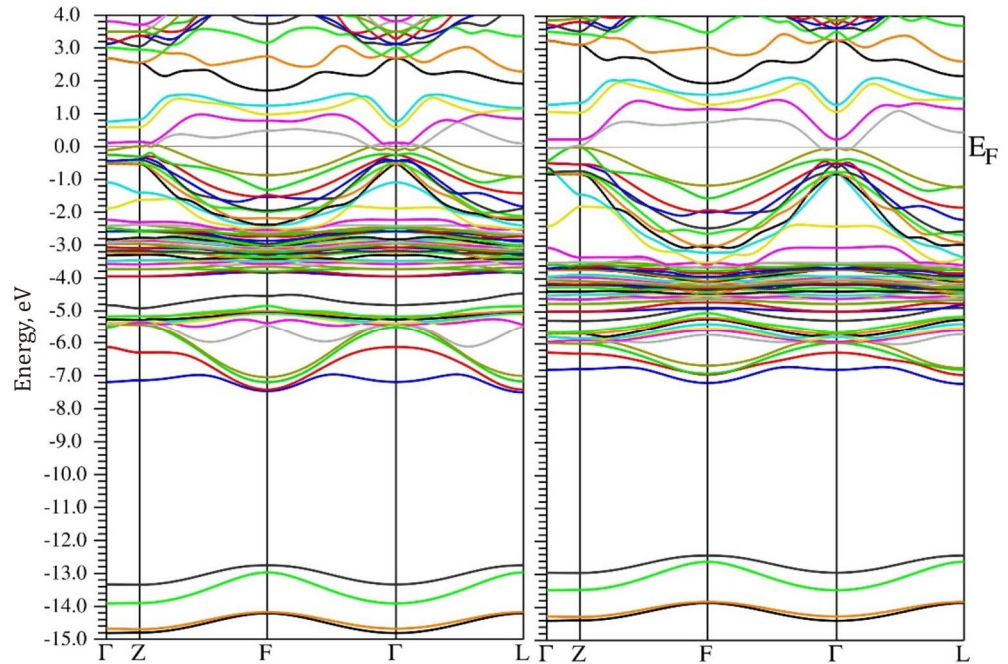
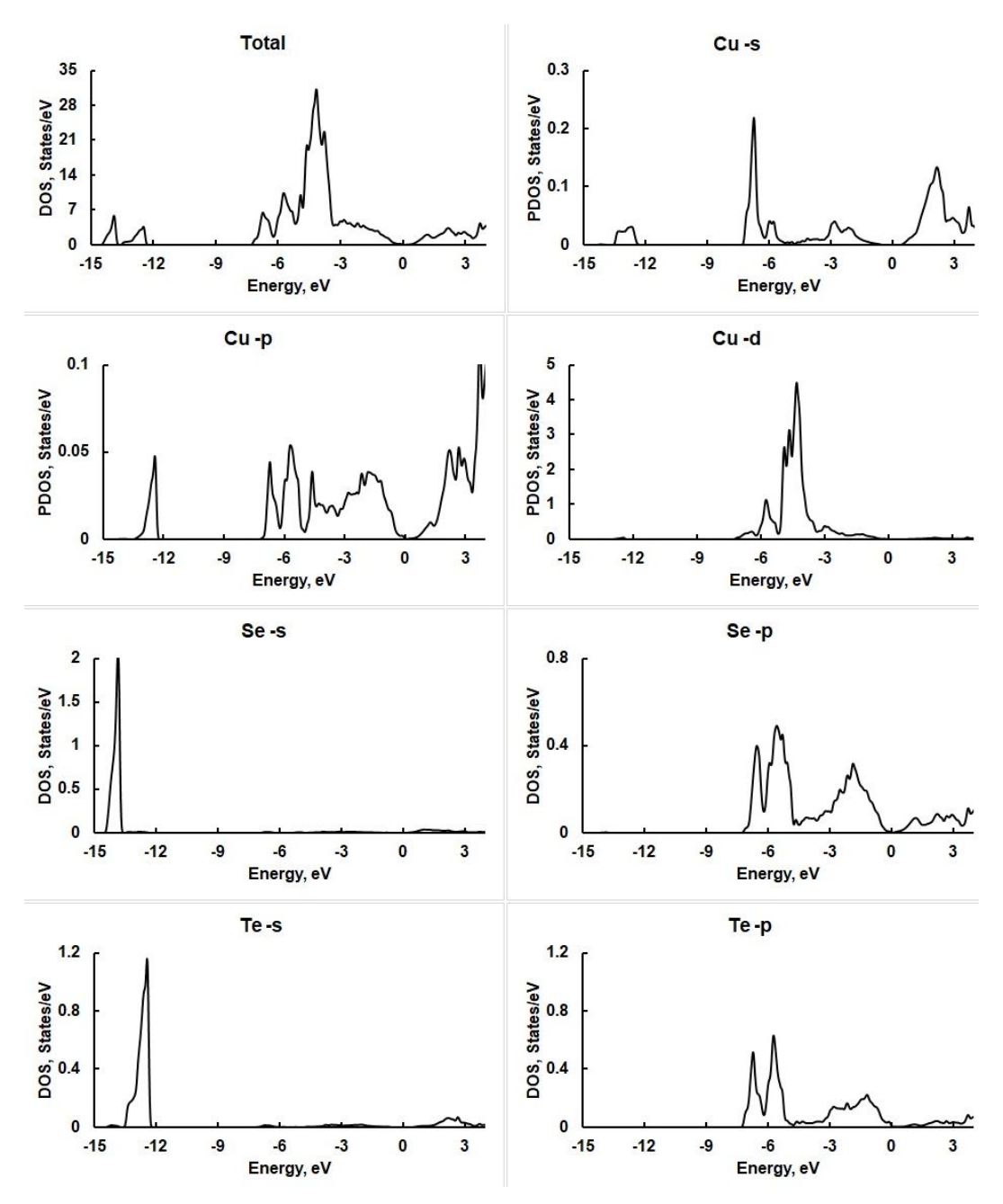


Fig. 2. Electronic band structure of  $Cu_4SeTe$  calculated using the GGA (left) and GGA+U (right) approximations.



**Fig. 3.** Total and atom-projected densities of states for Cu, Se, and Te atoms in Cu<sub>4</sub>SeTe. The Fermi level is aligned to zero energy.

The total and atom-projected densities of states (PDOS) are shown in Fig. 4. The lower part of the valence band (below –8 eV) is dominated by Se 4s and Te 5s orbitals, reflecting localized core-like states. The mid-valence region (–6 eV to 0 eV) mainly consists of Cu 3d states strongly hybridized with Se 4p and Te 5p orbitals. This hybridization indicates significant covalent bonding between Cu and the chalcogen atoms. Just above the Fermi level, the conduction bands are formed by Cu 4s and Se/Te p orbitals, resulting in delocalized states that dominate electrical conduction.

Such orbital contributions are essential for understanding interband transitions in the optical spectra. The optical absorption edge mainly results from transitions between the Cu 3d–Se/Te p states at the top of the valence band and the Cu 4s–Se/Te p states at the bottom of the conduction band. This accounts for the strong optical absorption in the 2–4 eV range seen in the calculated spectra. The GGA+U correction decreases the overlap of d- and p-states near the Fermi level. However, the overall semimetallic character and high density of states near the Fermi level remain, supporting efficient carrier generation and transport.

# 2.3. Influence on the thermoelectric and optoelectronic performance

The combined experimental transport measurements and theoretical electronic structure calculations provide consistent evidence that  $Cu_4SeTe$  is a semimetal with favorable characteristics for energy-related applications. Its electrical conductivity, Seebeck coefficient, and mobility place it between  $Cu_2Se$  and  $Cu_2Te$ , while its layered structure suggests reduced lattice thermal conductivity due to enhanced phonon scattering. This combination is beneficial for thermoelectric applications where a balance between high electrical conductivity and sufficient thermopower is essential.

From an optoelectronic perspective, the electronic band structure and PDOS show strong interband transitions involving Cu d- and Se/Te p-states, which cause intense optical absorption in the visible range. The calculated absorption coefficient reaches values around  $10^5$  cm<sup>-1</sup> between 2 and 4 eV, comparable to those of benchmark photovoltaic materials. Along with the optical anisotropy observed in the refractive index and extinction coefficient, these findings position Cu<sub>4</sub>SeTe as a promising candidate for thin-film solar cells and polarization-sensitive photodetectors.

#### 2.4. Optical functions

Fig. 4 presents the dependencies of the real and imaginary parts of the dielectric function  $\varepsilon(E)$  on the energy E for  $\mathrm{Cu_4SeTe}$  under different polarizations of incident light. The components  $\varepsilon_{\parallel}$  and  $\varepsilon_{\perp}$  correspond to the in-plane (parallel to the ab-plane) and out-of-plane (along with the c-axis) responses of the layered structure. The  $\mathrm{Im}\varepsilon$  spectra exhibit multiple pronounced peaks extending up to 8 eV, which are attributed to interband transitions from  $\mathrm{Cu}\ 3\mathrm{d} \to \mathrm{Cu}\ 4\mathrm{s}/4\mathrm{p}$  and  $\mathrm{Se}/\mathrm{Te}\ \mathrm{p}$  states, consistent with the electronic band structure and PDOS analysis. The presence of these peaks indicates strong light–matter interaction in the visible and near-UV regions.

The refractive indices n(E) and extinction coefficients k(E) are shown in Fig. 5. The refractive index decreases to approximately 3.1, while the extinction coefficient shows a

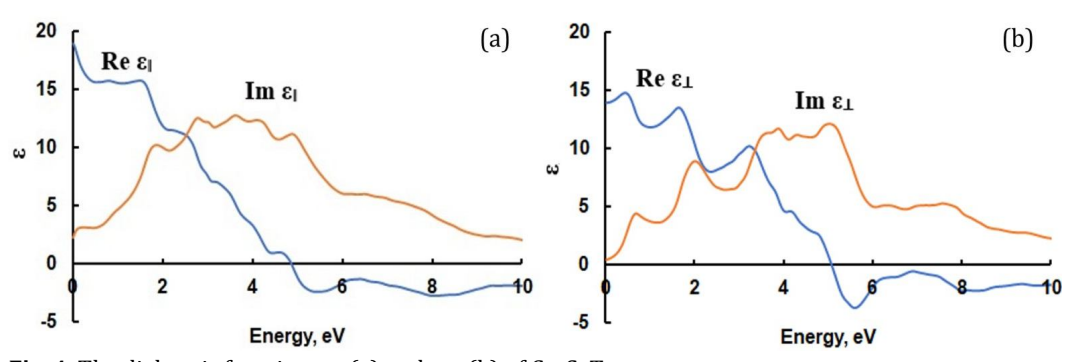


**Fig. 4.** The dielectric function  $\,arepsilon_{\parallel}\,$  (a) and  $\,arepsilon_{\perp}\,$  (b) of Cu<sub>4</sub>SeTe.

sharp rise beyond 1.2 eV, indicating the onset of strong absorption. This behavior reflects normal dispersion in the transparency region and follows the Kramers–Kronig relation between real and imaginary parts of the dielectric function. Around 5–6 eV, where the extinction coefficient k(E) reaches its maximum, the refractive indices exhibit a decrease with increasing photon energy, a hallmark of anomalous dispersion. This interplay confirms the correlation between absorption maxima and refractive index anomalies. The anisotropy in n (about 0.5 between  $n_{\parallel}$  and  $n_{\perp}$ ) is relatively strong and arises from the layered crystal structure of Cu<sub>4</sub>SeTe, where electronic transitions differ between in-plane and out-of-plane polarizations. The estimated numerical uncertainty of the refractive index and extinction coefficient values does not exceed 0.1 due to the chosen k-point mesh density.

Fig. 6 illustrates the reflection coefficients of  $Cu_4SeTe$  for both polarizations. The spectra display moderate reflectivity in the low-energy region, followed by enhanced reflection in the 3–5 eV range, in agreement with the strong absorption onset. Such reflectivity behavior is comparable to that of other layered chalcogenides and highlights the polarization dependence of the optical response.

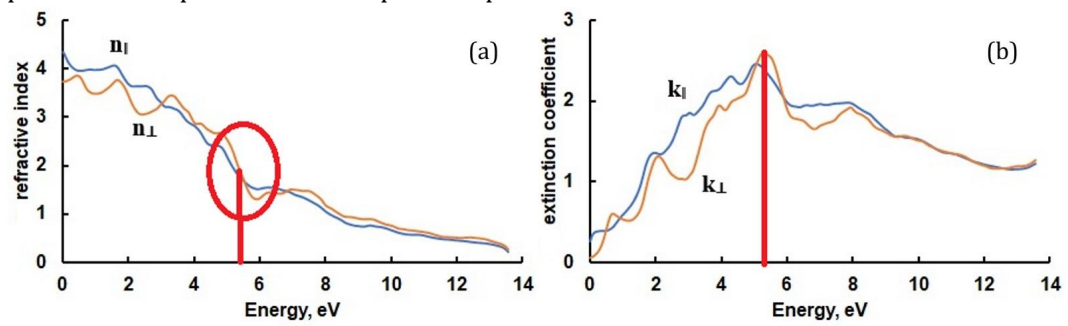


**Fig. 5.** The dependencies of refractive indices (a) and extinction coefficients (b) for in-plane and out-of-plane polarizations. A pronounced anisotropy ( $\sim$ 0.5 between  $n_{\parallel}$  and  $n_{\perp}$ ) is observed. n shows normal dispersion in the transparency region and abnormal dispersion near the 5–6 eV absorption maxima. Numerical uncertainty:  $\Delta n$ ,  $\Delta k \lesssim 0.1$ . The red line (panel (b)) corresponds to the range in which the extinction coefficient k(E) reaches its maximum, while the red circle (panel (a)) – to the range where the refractive indices exhibit the anomalous dispersion.

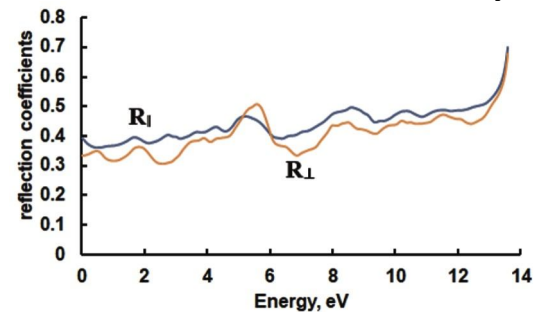


**Fig. 6.** Reflection coefficients of Cu₄SeTe for various polarizations of incident light.

The absorption coefficient spectra are shown in Fig. 7, with the *Y*-axis units corrected to cm<sup>-1</sup>. The calculated  $\alpha(E)$  reaches values of  $\sim 10^5 \text{cm}^{-1}$  in the 2–4 eV range, which is now explicitly visible in the revised plot. This absorption level is comparable to or exceeds that of benchmark photovoltaic and photodetector materials such as CdTe and Cu(In, Ga)Se<sub>2</sub>. A coefficient of this magnitude implies that nearly complete light harvesting can be achieved in films thinner than 1 micrometer, making Cu<sub>4</sub>SeTe particularly well-suited for thin-film device architectures. The high absorption coefficient, therefore, confirms that Cu<sub>4</sub>SeTe can act as an efficient absorber in optoelectronic applications requiring compact and lightweight active layers.

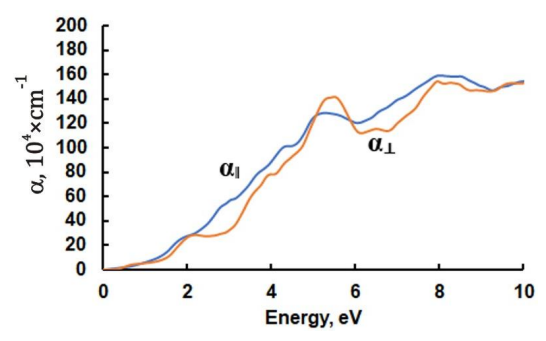
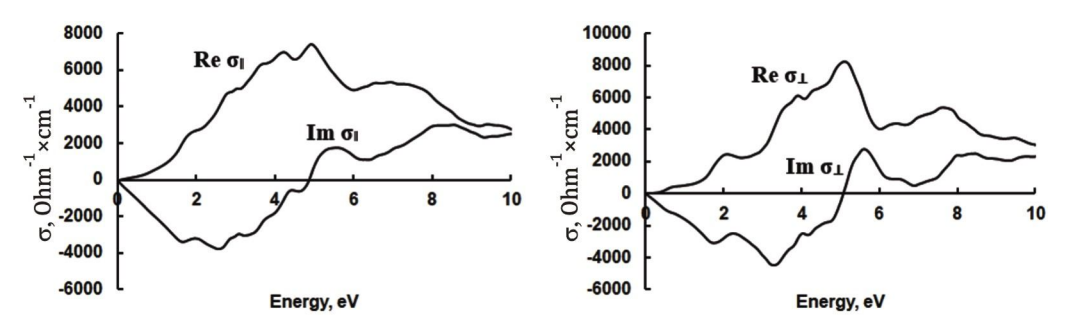


Fig. 7. Spectral dependence of the absorption coefficient  $\alpha(E)$  for Cu<sub>4</sub>SeTe under different polarizations of incident light.

Fig. 8 displays the spectral dependence of the real and imaginary parts of the complex optical conductivity. The pronounced peak in the real part of the optical conductivity,  $\sigma(E)$ , within the 2.5–5 eV energy range supports a strong electronic response in the visible spectrum. As depicted in Fig. 2 and 3, this energy region corresponds directly to the maximum in the density of states, which confirms the origin of this peak. The inclusion of dispersion of the imaginary part of conductivity further highlights the role of bound-bound electronic transitions and confirms the strong dispersive behavior in this energy region. The simultaneous analysis of real and imaginary parts of conductivity reveals a consistent picture in which strong interband excitations dominate the visible-to-UV spectral response.



**Fig. 8.** Spectral dependence of the real and imaginary parts of the complex optical conductivity of Cu<sub>4</sub>SeTe under different polarizations of incident light.

Taken together, these optical properties establish a direct connection between the electronic structure and the macroscopic optical response of  $Cu_4SeTe$ . The agreement between  $\varepsilon(E)$ , n(E), k(E),  $\alpha(E)$ ,  $\sigma(E)$ , and the calculated PDOS underscores the robustness of the results and the predictive power of the first-principles approach. Importantly, the combination of high absorption, significant optical anisotropy, and correlated interband transitions positions  $Cu_4SeTe$  as a multifunctional material. Its high absorption coefficient supports thin-film photovoltaic applications, while the polarization dependence of n and k suggests potential in polarization-resolved photodetectors, optical filters, and waveguide-integrated sensors. In addition, the broadband response and semimetallic character make  $Cu_4SeTe$  a promising candidate for thermophotovoltaic converters and other energy-harvesting technologies.

To contextualize the physical properties of Cu<sub>4</sub>SeTe, Table 1 offers a comparative overview of the structural, electrical, and optical parameters of Cu<sub>2</sub>Se, Cu<sub>2</sub>Te, and Cu<sub>4</sub>SeTe. The comparison emphasizes the intermediate nature of Cu<sub>4</sub>SeTe regarding conductivity and Seebeck coefficient. Notably, the available data indicate that Cu<sub>4</sub>SeTe could serve as a promising multifunctional material bridging binary copper chalcogenides.

Table 1. Comparative structural and electrical properties of Cu<sub>2</sub>Se, Cu<sub>2</sub>Te, and Cu<sub>4</sub>SeTe

Parameter	Cu <sub>2</sub> Se	Cu <sub>2</sub> Te	Cu₄SeTe
Space group	Fm 3 m (cubic) [7]	Pnma / $P\overline{3}$ m1 (orthorhombic / trigonal) [8]	R $\overline{3}$ m (trigonal) [12]
Measurement temperature range, K	300-800 [7,13]	300–700 [8]	80-320 [12]
Electrical conductivity, S/cm	~500–2000 [7,13]	~300-1000 [8]	~720 at 300 K (this work)
Hole mobility, cm <sup>2</sup> /V⋅s	~30-40 [7]	~15-25 [8]	~20 (this work)
Seebeck coefficient, μV/K	~180-220 [7,13]	~150-200 [8]	~170 (this work)
Conductivity type	p-type [7,8]	p-type [8]	p-type (this work)
Absorption coefficient $\alpha$ , cm <sup>-1</sup>	10 <sup>5</sup> –10 <sup>6</sup> (visible range) [9]	104–105 [9]	$\sim 10^5$ (2-4 eV range, this work)

Overall,  $Cu_4SeTe$  combines the features of  $Cu_2Se$  and  $Cu_2Te$  while providing added tunability through its mixed-anion composition. Its distinctive blend of semimetallic behavior, strong optical transitions, and structural anisotropy emphasizes its potential as a next-generation optoelectronic material worthy of further theoretical and experimental investigation.

#### 3. Conclusions

In this work, the electronic structure and optical properties of the ternary compound  $Cu_4SeTe$  are systematically examined using first-principles density functional theory. The results show a semimetallic electronic character, with the valence band mainly influenced by Cu 3d and Se/Te p orbitals. Conversely, the conduction band mostly consists of Cu 4s and Se/Te p states. This orbital hybridization creates a high density of states near the Fermi level, enabling strong interband transitions.

The calculated optical spectra demonstrate strong light-matter interactions in the visible-to-near-UV range. In particular, the absorption coefficient  $\alpha(E)$  reaches values around  $10^5$  cm<sup>-1</sup> between 2 and 4 eV, while the optical conductivity  $\sigma(E)$  shows prominent peaks in the 2.5–5 eV region. These results establish Cu<sub>4</sub>SeTe as a strong absorber well-suited for thin-film optoelectronic devices such as solar cells, photodetectors, and thermophotovoltaic converters. The observed optical anisotropy further indicates potential for polarization-sensitive applications like integrated waveguide sensors and optical filters.

Compared to the binary phases  $Cu_2Se$  and  $Cu_2Te$ , the ternary  $Cu_4SeTe$  phase combines beneficial features of both, connecting their functionalities while adding more tunability through its mixed-anion composition. This combination of semimetallic transport, high absorption efficiency, and anisotropic optical response makes  $Cu_4SeTe$  a promising multifunctional material for future energy conversion and optoelectronic applications.

Future research should focus on the role of dopants, intrinsic defects, and nanostructuring in controlling the electronic and thermal transport properties of Cu<sub>4</sub>SeTe. Additionally, experimental investigations of its optical response, carrier dynamics, and thermal conductivity are essential for validating the theoretical predictions and fully evaluating the material's potential in advanced device applications.

**Conflict of Interests.** The authors declare that they have no conflicts of interest, whether financial or personal, that could have influenced the work reported in this paper.

**Funding.** This research received no funding.

### References

- 1. Sakuma, T., Sugiyama, K., Matsubara, E., & Waseda, Y. (1989). Determination of the Crystal Structure of Superionic Phase of Cu2Se. *Materials Transactions, JIM, 30*(5), 365-369.
- 2. Heyding, R. D., & Murray, R. M. (1976). The crystal structures of  $Cu_{1.8}Se$ ,  $Cu_3Se_2$ ,  $\alpha$ -and  $\gamma CuSe$ ,  $CuSe_2$ , and  $CuSe_2$  II. Canadian Journal of Chemistry, 54(6), 841-848.
- 3. Yamamoto, K., & Kashida, S. (1991). X-ray study of the average structures of Cu2Se and Cu1. 8S in the room temperature and the high temperature phases. *Journal of Solid State Chemistry*, 93(1), 202-211.
- 4. Yu, B., Liu, W., Chen, S., Wang, H., Wang, H., Chen, G., & Ren, Z. (2012). Thermoelectric properties of copper selenide with ordered selenium layer and disordered copper layer. *Nano Energy*, 1(3), 472-478.
- 5. Liu, H., Shi, X., Xu, F., Zhang, L., Zhang, W., Chen, L., Li, Q., Uher, C., Day, T., & Snyder, G. J. (2012). Copper ion liquid-like thermoelectrics. *Nature Materials*, 11(5), 422-425.
- 6. Morimoto, N., & Koto, K. (1966). Crystal structure of umangite, Cu<sub>3</sub>Se<sub>2</sub>. Science, 152(3720), 345-345.
- 7. Bychkov, E. (2009). Superionic and ion-conducting chalcogenide glasses: Transport regimes and structural features. *Solid State Ionics*, 180(6-8), 510-516.
- 8. Gabor, A. M., Tuttle, J. R., Albin, D. S., Contreras, M. A., Noufi, R., & Hermann, A. M. (1994). High-efficiency CuIn<sub>x</sub>Ga<sub>1-x</sub>Se<sub>2</sub> solar cells made from (In<sub>x</sub>, Ga<sub>1-x</sub>)<sub>2</sub>Se<sub>3</sub> precursor films. *Applied Physics Letters*, *65*(2), 198-200.
- 9. Shen, J., Liu, H., & Li, Y. (2024). A way to identify whether a DFT gap is from right reasons or error cancellations: The case of copper chalcogenides. *The Journal of Chemical Physics*, 160(24).
- 10. Guerroum, J., Al-Hattab, M., Moudou, L., Rahmani, K., Lachtioui, Y., & Bajjou, O. (2025). Structural, electronic, and optical studies of chalcogenides stannite  $Cu_2CdSnX_4$  (X= S, Se, and Te): insights from the DFT study. Optoelectronics Letters, 21(2), 69-76.
- 11. Zhou, Z., Huang, Y., Wei, B., Yang, Y., Yu, D., Zheng, Y., Zou, M., Lan, J-L., He, J., Nan C-W. & Lin, Y. H. (2023). Compositing effects for high thermoelectric performance of  $Cu_2Se$ -based materials. *Nature Communications*, 14(1), 2410.
- 12. Amiraslanov, I. R., Azizova, K. K., & Aliyeva, Y. R. (2017). Crystal structure of Ga<sub>4</sub>SeTe. *Crystallography Reports*, 62(2), 215–218.
- 13. Blaha, P., Schwarz, K., Madsen, G. K. H., Kvasnicka, D., & Luitz, J. (2008). WIEN2k: An augmented plane wave + local orbitals program for calculating crystal properties. Vienna University of Technology.

Azizova, K. K., Jahangirli, Z. A., Ragimov, S. S., Nurubeyli, T. K., Suleymanova, L. Ch., Kerimli, N. V., Mammadova, G. N., Mammadov, L. V., Gulieva, S.O. (2025). *Ab Initio* Calculations of the Electronic Structure and Optical Properties of Cu<sub>4</sub>SeTe Crystals. *Ukrainian Journal of Physical Optics*, *26*(4), 04049–04057. doi: 10.3116/16091833/Ukr.J.Phys.Opt.2025.04049

**Анотація.** У цій роботі ми представляємо комплексне теоретичне дослідження електронної структури та оптичних властивостей кристалів Си<sub>4</sub>SeTe з використанням розрахунків за допомогою теорії функціоналу густини (DFT), з перших принципів. Аналіз охоплює зонну структуру, повну та часткову густину станів (DOS та PDOS), комплексну діелектричну функцію, показник заломлення, коефіцієнт екстинкції, відбивну здатність, коефіцієнт поглинання та оптичну провідність. Результати показують, що Си<sub>4</sub>SeTe поводиться як напівметал з гібридизованими станами Си 3d та Se/Te р, що домінують у валентній області, тоді як стани Си 4s та Se/Te р формують зони провідності. Розраховані оптичні спектри демонструють сильне поглинання у видимому діапазоні (2–4 eB), з коефіцієнтами поглинання, що досягають приблизно 105 см¹, разом із помітними міжзонними переходами та суттєвою оптичною анізотропією. Ці результати свідчать про те, що Си<sub>4</sub>SeTe є перспективним багатофункціональним матеріалом з потенційним застосуванням у тонкоплівкових фотоелектричних елементах, фотодетекторах та термоелектричних пристроях.

**Ключові слова:** Си₄SeTe, ab initio розрахунки, оптичні властивості, густина станів, діелектрична функція, коефіцієнт поглинання, відбивна здатність